2nd International Symposium on Magnetic Beaing
July 12-14, 1990, Tokyo, Japan

LOADING TEST IN AN AIR TURBINE BORNE BY ACTIVE MAGNETIC BEARINGS

T. INOUE*, M. TAKAGI*, N. TAKAHASHI*, O. MATSUSHITA* and R. KANEKO**
* Mechanical Engineering Research Laboratory , Hitachi Ltd.
** Hitachi Works , Hitachi Ltd.
3-1-1 Saiwai-machi, Hitachi-shi, Ibaraki Pref. 317, JAPAN

Abstract

A conventional air turbine with a load capability of 82 KW is modified with the installation of active magnetic bearings, and loading tests are then performed. The controller unit is constituted by phase compensators and PWM power amplifiers. The phase compensator is principally based upon the conventional PID control law with the addition of several notch filters, which enable the prevention of self-excited oscillations in the bending mode eigen frequencies. During rotational tests, rotor vibration is successfully suppressed to less than 40 μm amplitude. The loading tests are conducted normally without malfunctions in either the analog controller or the digital controller.

1. Introduction

Active magnetic bearings, which have been applied to such compact-size rotary machines as spindles and turbomolecular pumps up until the present time, have recently been applied to such turbomachines as centrifugal compressors. Magnetic bearings are attracting much attention as a mechanical element to be used in place of conventional oil-film bearings for turbomachines, of which maintenance-free operation is very important. Magnetic bearings, having low bearing loss without lubrication, can also contribute towards improvement of fluid performance. Magnetic bearings are now being applied particularly to centrifugal compressors, with subsequent reports written about their operation [1]. It seems, however, that such reports do not have detailed descriptions of what characteristics are realized in the controller, which forms the key to the control of vibrations with electromagnetic bearings. Moreover, while examples of digital control with a model rotor [2] are reported occasionally, it appears that reports concerning turbomachines indicate a controller constructed in an analog circuit with no report yet on test results of turbomachines with digitally controlled electromagnetic bearings.

Therefore, this report presents in detail the vibration characteristics of the shaft system, characteristics of the analog and digital controllers, the open loop transfer function of the entire controlling system, and so forth. These are ascertained in light of tests conducted on a performance test machine formed of an air turbine with electromagnetic bearings. Additionally, a description of the results obtained from the rotational test, the loading test, and the partial loading test.

2. Test rig

2.1 Air turbine with electromagnetic bearings

The schematic construction of the air turbine with electromagnetic bearings subjected to a series of tests is shown in Fig. 1. The turbine rotor is set with a shrink-fit disk in one stage having a diameter of 600 mm. The weight of the rotor is 3.2 kN and the bearing span is 1,060 mm. The turbine rotor is connected by a diaphragm coupling directly with an electric dynamometer rated at the output capacity of 100 kw. However, this rotor is not provided with a damper unit which prevents the occurrence of higher order vibrations. One end of the radial magnetic bearing is set inside the air turbine casing, while the other end is held in the pedestal provided between the turbine casing and the dynamometer. A thrust bearing is also set in this pedestal. Touch bearings are provided in two places on the left side and the right side in order to protect the turbine rotor in the event of trouble occurring in the magnetic bearings.

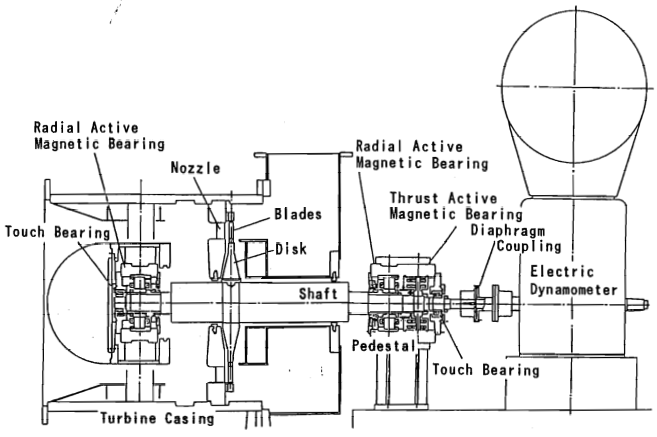

Fig. 1 An air turbine borne by active magnetic bearings

The working air is fed with a blower rated at 600 kw in output. The air flows into the blower from the left and is ejected through the nozzle, turning the turbine blades and being discharged in the upward direction. The turbine has the specified revolutions of 3,600 rpm, with its over-revolution limit set at 4,320 rpm.

The relation between the natural frequency of this rotor system and the spring constant of the magnetic bearings is shown in Fig. 2. The natural frequency which shows a considerable change in relation to the spring constant, occurs in the rigid body mode, in which the rotor oscillates in parallel and in conical modes. On the other hand, the natural frequency in the shaft bending mode shows almost no change, even if the spring constant of the bearings changes. The natural frequency in the shaft bending mode is 210 Hz in the primary value and 440 Hz in the secondary value. Now that the specified revolutions are 3,600 rpm, it is sufficient to pass the two critical speeds of the rigid body, and it is not necessary to pass the critical speed for the primary value in the bending mode.

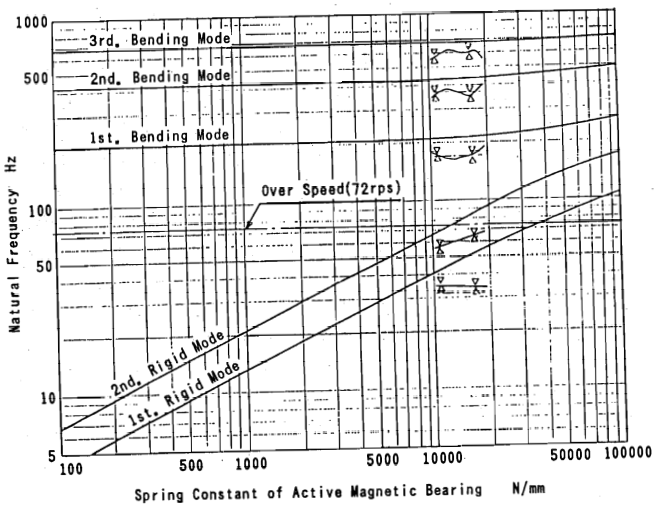

Fig. 2 Natural frequency of the rotor

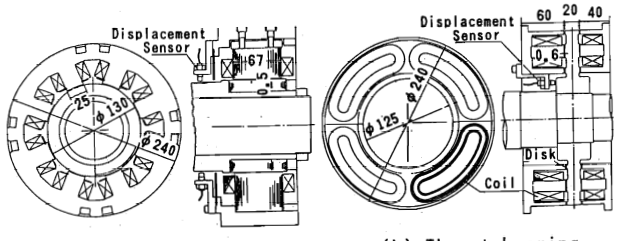

(a) Radial bearing (b) Thrust bearing

Fig. 3 Active magnetic bearing

2.2 Magnetic bearings

2.2.1 Magnetic radial bearings

The magnetic radial bearings are designed with the design radial load set at 2 kN in consideration of the weight of the rotor and the dynamic load, and with the magnetic flux density in the air gap of the magnetic bearings set at 1 T. The construction of the magnetic bearings, as shown in Fig. 3 (a), measures 240 mm in the outer diameter, 130 mm in the inner diameter, 67 mm in the bearing width, and 0.5 mm in the bearing air gap and is formed with a total number of eight magnetic poles. The core is made of a 3% silicon steel sheet with a thickness of 0.5 mm, as laminated in a total of 134 sheets. The magnetic coils are formed of conductive wire with a diameter of 2mm, and with the coil winding in 60 turns. These coils are connected in a series.

2.2.2 Magnetic thrust bearings

The magnetic thrust bearings are designed with the design thrust load set at 10 kN in consideration of the fluid force, and with the magnetic flux density set at 1 T. Their construction, shown in Fig. 3 (b), measures 240 mm in the outer diameter, 125 mm in the inner diameter, 60 mm in bearing length on the loaded side and 40 mm in the bearing length on the opposite side, 0.6 mm in the thrust air gap, and has a total of four magnetic poles. The core is made of low carbon steel. The magnetic coils are made of a conductive wire with a diameter of 1.6 mm wound in a total of 154 turns in the formation of the coil winding. Four such coils are connected in a series.

2.3 Displacement sensor

Eddy current sensors are used as the displacement sensors to detect the position of the rotor shaft core. They are provided opposite each other on the X-axis and the Y-axis. With a form of differential input used for the sensors, temperature drift in the DC output from the displacement amplifier is suppressed, by preventing such external disturbances as changes in temperature. The stability at the point of static equilibrium of the shaft core is thereby secured.

2.4 Controllers

The phase compensation is done by the PID process, performed with the analog controller, which is formed of an operating amplifier, and, with the digital controller composed of TMS 320C25, a DSP made by TI Co. This is shown in Fig. 4. The sampling frequency is 8 kHz. A 12-bit analog-digital converter and a 12-bit digital-analog converter are employed for the input and the

output. Moreover, the PWM system, which attains high efficiency at a low level of heat generation, is used for the power amplifier for feeding an electric current to the magnetic coils. The amplifier has a capacity of 20 kVA for operation at the maximum voltage of 200 V and the maximum current of 20 A per channel.

3. Calculation of stability in control system

Prior to the tests, an analysis of the stability of the rotor and the entire control system was made, with software [3] developed by the present writers and some associates, with a view to simplifying the tuning of the controllers. The block diagram of the control system as a whole, with a notch filter included in the PID, is shown in Fig. 5. The shaft position is detected by the displacement sensor, and the signal generated by the sensor is input into the controllers. The signal is processed for its phase compensation by the proportioning unit, the integrating unit, and the differentiating unit, via the low pass filter at the first stage. Then, the signal is given a further phase compensation by the notch filter with a central frequency almost in agreement with the primary natural frequency and the secondary natural frequency of the shaft. The PWM power amplifier is driven, which feeds an electric current to the magnetic coils, thereby controlling the rotor.

The results obtained from the calculation of the stability of each eigen value in the control system are presented in Fig. 6. The horizontal axis represents the frequency, while the vertical axis indicates the damping ratio. It is observed that the natural frequencies in the primary rigid body mode and the secondary rigid body mode have high damping ratios, so that they offer favorable controllability. The damping factors for the primary and secondary natural frequencies become negative, so that these natural frequencies cause vibrations if the notch filters are not included. On the other hand, it is seen that the damping ratios of these natural frequencies become positive, attaining a state of stabilization, when the notch filters are included. In this figure, the natural frequency with a damping ratio in the proximity of 1 forms the pole for the electrical circuit system.

4. Test results

4.1 Characteristics of control system

4.1.1 PID controller

The transfer functions of the PID controller in the analog control system for radial vibrations are shown in Fig. 7 (a). This Figure

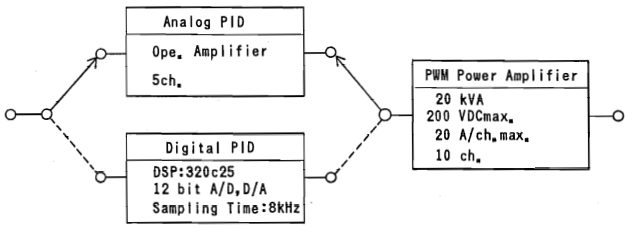

Fig. 4 Controllers

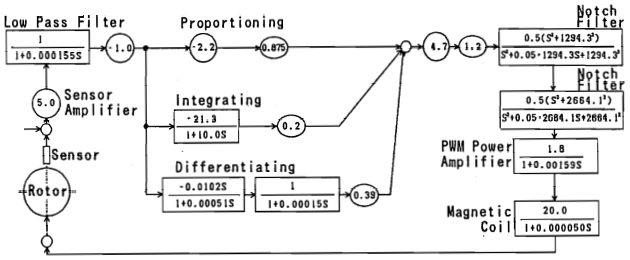

Fig. 5 Block diagram of the entire control system

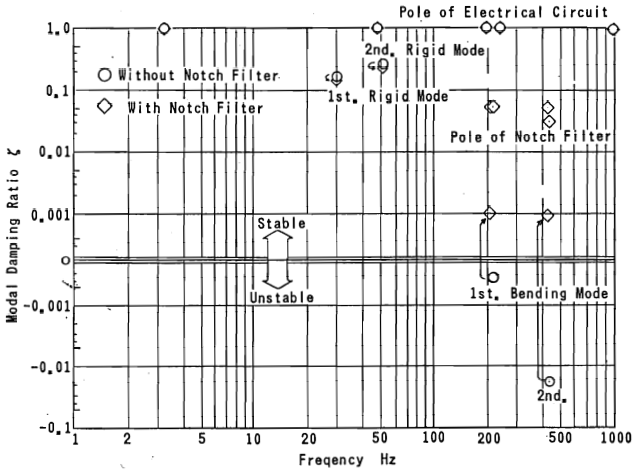

Fig. 6 Results of stability analysis

shows differential characteristics with the gain remaining almost flat up to 20 Hz and incrementing in a monotonous pattern. Moreover, for the purpose of preventing the oscillation of bending modes, notch filters are set up at 200 Hz and 425 Hz in correspondence with the primary and secondary natural frequencies at 210 Hz and 440 Hz in the bending mode. The frequency in the notch filter is set at a level somewhat lower than the natural frequency of the shaft system because the system will not fall into an unstable state even if the natural frequency changes to some extent in the course of its rotation as the frequency has a phase lead in the high frequency region while it has a lag in the phase in the frequency region lower than the notching frequency,

as is clearly observed in the phase characteristics chart. The minor phase delay in the lower frequency region is due to the performance of integrating operations for preventing a steady-state deviation. This presents no problem, since the time constant in the integrating unit is set at a sufficient length.

The transfer functions for the PID controller in the digital control system are shown in Fig. 7 (b). As is evident in comparison with Fig. 7 (a), the digital controller attains approximately the same gain and phase characteristics as those of the analog controller. The notching characteristics of the notching filters in this system are the same as those of the analog controller. It is possible to perceive the accuracy and expediency of the digital controller, which can be constructed through the medium of software. This controller is extremely effective for simplified tuning. Owing to the sampling frequencies set as high as 8 KHz for the analog-digital conversion and digital-analog conversion, the system can amply secure the necessary phase characteristics in the high frequecy region even if it performs arithmetic operations with the PID to the extent just described.

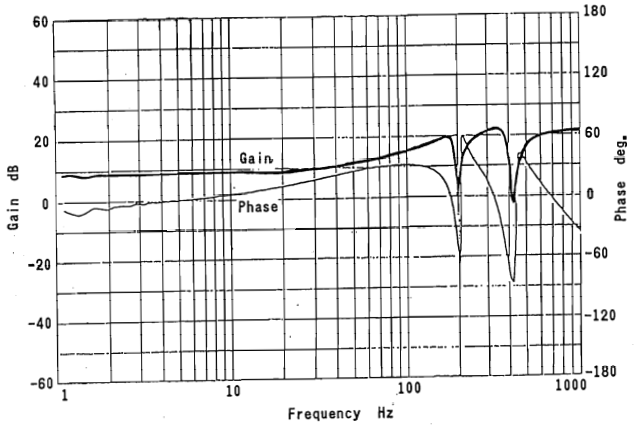

(a) Analog controller

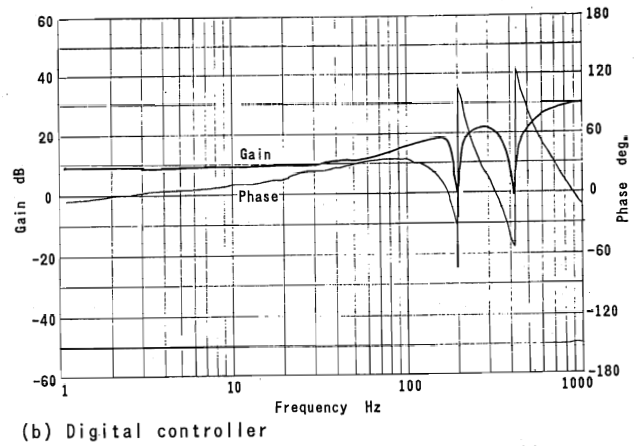

(b) Digital controller

Fig. 7 Transfer function of PID controller

4.1.2 Open loop transfer function

The open loop transfer function of the entire radial control system is presented for the analog control system in Fig. 8 (a) and for the digital control system in Fig. 8 (b). In the analog control system, the gain characteristics show a decline, along with a rise in frequency, and have small peaks at 100 Hz, 210 Hz, and 440 Hz. In this regard, the peak at 100 Hz reflects the natural frequency of the pedestal while the other peaks correspond to the natural frequencies of the bending modes in the shaft system. As the gains at these bending natural frequencies are held down to the order of -15 dB, it is found that the characteristics just described will not cause any vibrations and will have a high degree of latitude to the fluid vibrating force. Also, the phase characteristics feature a lead in phase

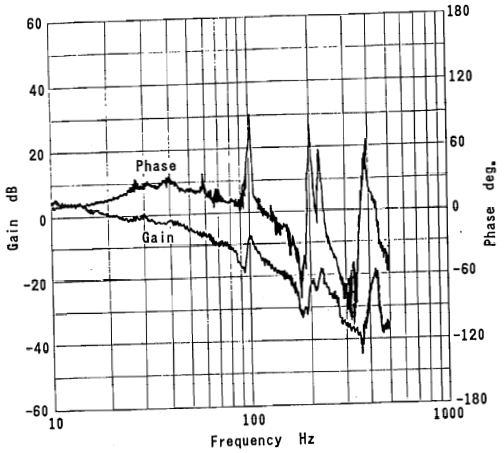

(a) Analog controller

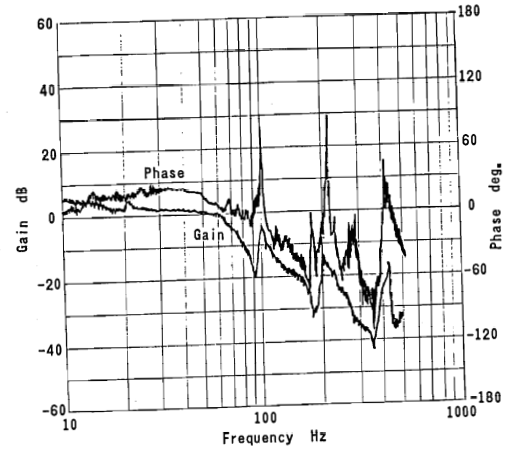

(b) Digital controller

Fig. 8 Open characteristics of the entire control system

up to 130 Hz, and thus it is observed that the characteristics leave an ample margin in reserve for 60 rps, which is the rated speed of this equipment.

The open loop transfer function of the digital control system, as presented in Fig. 8 (b), has small differences either in the gain or the phase characteristics. This control system achieves slightly less phase compensation, with a lead in phase up to 80 Hz, in comparison with the analog control system. In the digital control system, an unavoidable quantizing error takes place when the sensor signals are turned into digital signals by the analog-digital converter. The resulting noises exert vibration in the rigid body mode of the shaft system, thereby causing residual vibrations. Therefore, the gain from the differential operation in this system has been set at a smaller value than in the analog system. However, even at this level of phase compensation, the system has an ample margin of controlling capacity for the rated speed, 60 rps. Hence, there is no problem arising from this.

4.1.3 Free vibration waveforms

Fig. 9 illustrates the free vibration waveforms as measured by an impulse vibrating method applied to the analog control system at a time when the rotor is at a standstill. The radial vibration in the magnetic bearing on the left side is shown in Fig. 9 (a), which radial vibration in the magnetic bearing on the right side is shown in Fig. 9 (b), and the thrust vibration in the axial direction of the rotor is shown in Fig. 9 (c). All these free vibration waveforms are damped after showing approximately four peaks in each, and the damping ratios are at a high level, ranging from 0.3 to 0.5. On the basis of the frequency analysis results, it is found that the natural frequency in the primary rigid body mode is 22 Hz, and in the secondary rigid body mode is about 46 Hz although it is not distinctly discernible, as the peaks are so small in reflection of the high damping ratio. The natural frequency in the axial direction is 20 Hz.

4.2 Rotational test

The shaft vibration responses controlled by the analog system and the digital system, under a no load operation are shown in Fig. 10 (a) and Fig. 10 (b), respectively. On the basis of the vibration responses, it is observed that the critical speed in the primary rigid body mode is at 1,300 rpm (22 Hz). On the other hand, the peak of the critical speed in the secondary rigid body mode, which is not distinctly recognizable, is considered to be in the proximity of 2,800 rpm (46 Hz), as judged in light of the results of the impulse test. The vibration amplitude is approximately 40 μm at most even at the critical speed in the primary rigid body mode, and is 20 μm in the proximity of the rated speed, thus achieving stable vibration characteristics. Yet, the shaft vibration shows a tendency towards its increase at 4,320 rpm (72 Hz), which is an overspeed of 120 %. This is due to an increase occurring in the natural frequency component in the primary bending mode. This increase occurs because a vibrating component three times as large as the rotating frequency N (72 x 3 = 216 Hz), has coincided with the natural frequency of the shaft in the primary bending mode. This tendency is also observed in the form of small peaks in 5N at 2,700 rpm (45 Hz), and in 4N at 3,240 rpm (54 Hz), although these peaks occur at a smaller vibration level.

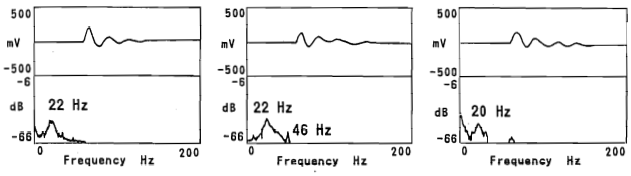

(a) Radial(X_1) (b) Radial(X_2) (c) Axial(Z)

Fig. 9 Free vibration and natural frequency

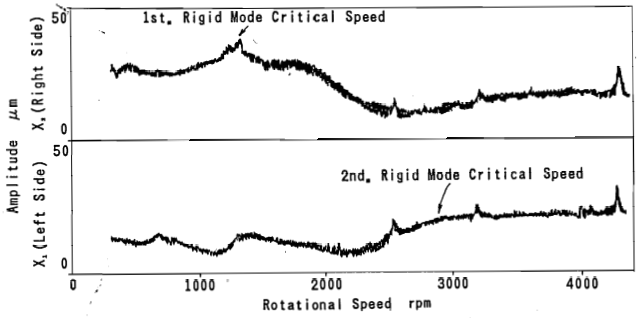

(a) Analog controller

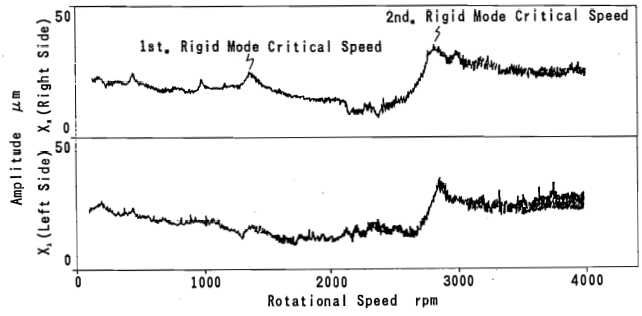

(b) Digital controller

Fig. 10 Rotor vibration response

These states are evident from the spectra of vibrations at the time of rotation, as shown in Fig. 11. The spectrum of vibration at 2,700 rpm shows an example of the coincidence of the vibrating component five times as large as the rotating frequency N with the natural frequency in the primary bending mode. However, the natural frequency components in the primary and secondary bending modes are not observed either at 3,000 rpm or at 3,600 rpm. As it can be estimated from the results described above, it is not sufficient merely to reduce the gain at the higher-order natural frequencies in the shaft bending mode by means of a notch filter. It is in fact important to also maintain a lead in phase in the case of a controller for turbomachines, in which the vibrating force at the degrees of revolution tends to grow larger. For this reason, the frequency in the notch filter is set at a level somewhat lower than the natural frequency of the shaft system. However, the actual tuning job requires much trouble because the natural frequency of the shaft at the time of its revolution deviates from that at the time of its standstill under the influence of the gyro effect. In order to perform the tuning work with high efficiency, taking account of the phase characteristics, it is essential to utilize software for analysis, and the present authors are planning to report on an example [4] of simulations with such software.

The shaft vibration response in Fig. 10 (b) on the unloaded operation of the digital control system shows a somewhat larger amplitude of vibration at the critical speed in the secondary rigid body mode in comparison with that in the analog control system. However, since the amplitude of vibration is on the order of approximately 50 μ m, which marks a fully permissible value, it can be stated that the digital control system has achieved its controlling performance at a level comparable with that of the analog control system. In view of such factors as the simplicity and convenience in tuning and the period necessary for the development work, it can be stated that the digital control is better than the analog control for its use as a controller for magnetic bearings.

4.3 Loading test

Shaft vibration characteristics in which the condition that the loading torque applied to the turbine is increased step by step at 2,000 rpm are shown in Fig. 12. When a load is placed on the turbine, the shaft vibrations in the positions of the two radial bearings show constant values

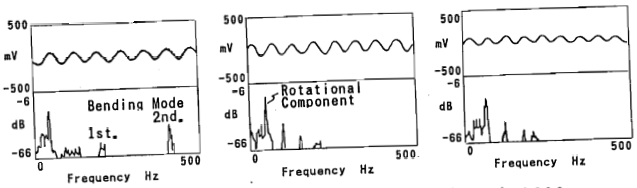

(a) 2700 rpm (b) 3000 rpm (c) 3600 rpm

Fig. 11 Spectra of vibrations at the time rotation

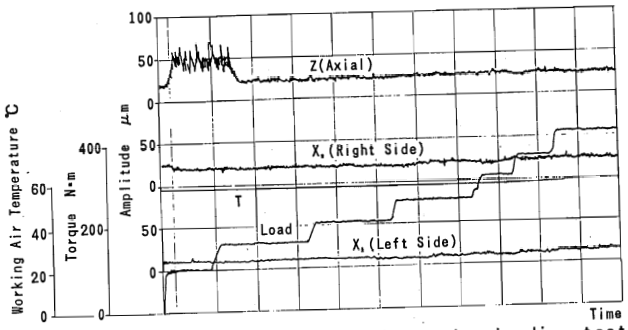

Fig. 12 Vibration characteristics under loading test

regardless of the load. In contrast to this, there appeared a phenomenon marked by a sharp increase of vibrations in the axial direction two times, from 25 μ m to 50 μ m, in terms of the amplitude of vibration under the loading torque of 10 kgf·m. Moreover, as the testing revolutions increased, this phenomenon began to occur on the higher loaded side, but did not occur at 4,000 rpm, where the load became still larger.

Therefore, inquiries were made into the relationship among the load and the current measured by the radial bearings (the radial load), and the thrust bearings (thrust load), at the individual revolutions specified for the test. The results obtained from the study relate to the case of ordinary ejection as shown in Figs. 13 (a) and (b). While the radial bearing current shows a declining tendency in relation to the increase in the output from the turbine, its rate of change is minimal. In contrast to that, the thrust bearing current is placed under the effect of a reverse thrust load in relation to the flow of air when the output from the turbine is low, but is subjected to the effect of a thrust load in the direction of the air flow when the output from the turbine grows larger. That is to say, it is found that the vibration in the axial direction increases sharply with the turbine output at which the thrust load becomes zero by the effect of a reversal in the direction of the thrust load. As no bias current is applied to the magnetic thrust bearings employed for this equipment, the

spring constant of the magnetic thrust bearings will become extremely small under the load condition which reduces the thrust load to zero. Then, the natural frequency in the axial direction decreases, falling into the phase delay zone (differential characteristics) in the lower frequency region for the controller, so that the thrust bearing current becomes unstable.

Therefore, in a turbomachine like this air turbine in which the the thrust load sometimes becomes zero upon the reversal of the direction of the thrust load by the effect of the fluid force, it is necessary to provide an ample flow of bias current, thereby suppressing the fluctuations otherwise likely to occur in the thrust rigidity.

4.4 Partial loading test

The relationship among load applied in the partial loading test, the radial bearing current (radial load), and the thrust bearing current (thrust load) are shown in Figs. 13 (a) and (b). The partial load was simulated by covering one third of the injection nozzle with a shield plate when the rotor was in its counterclockwise rotation, as shown in the figures. In

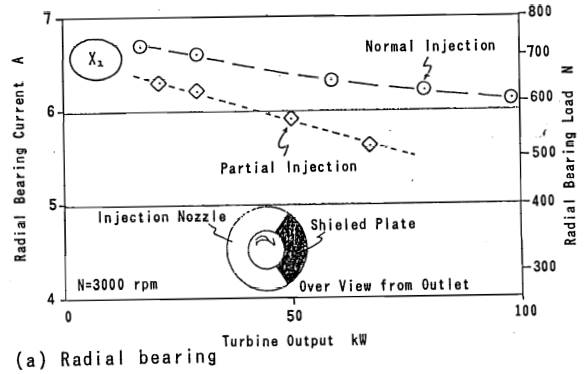

(a) Radial bearing

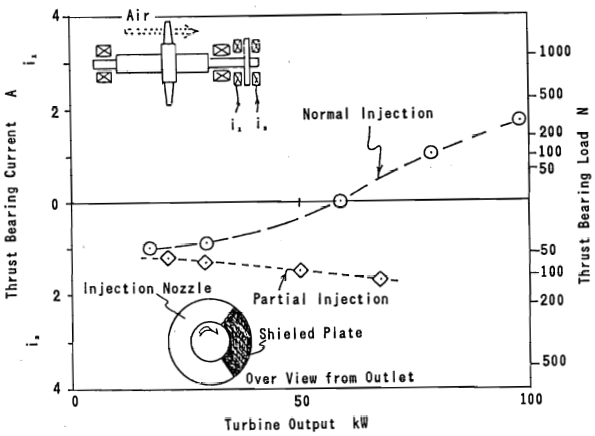

(b) Thrust bearing

Fig. 13 Active magnetic bearing loads

the case of such partial injection, the fluid force tending to push the rotor upward is at work, and the load on the radial bearings decreases as compared with the load at the time of the normal injection. In respect of the increase in the output from the turbine, the same tendency as at the time of the normal injection is observed. Although the thrust load reverses the loading direction in the case of the normal ejection, as mentioned above, the loading direction does not change in the partial injection. As discussed so far, it is considered one of the merits of magnetic bearings with no parallel in the conventional bearings, that it is possible to gain an accurate measure of the fluid force through the measurement of the coil current in the magnetic bearings.

5. Conclusion

With a machine formed by modifying the oil-film bearings into magnetic bearings in a conventional air turbine performance test rig, inquiries were made into the vibration characteristics of the shaft system and the open loop transfer function of the entire control system. A comparison was also made of the control performance of an analog controller and a digital controller of the PID system through rotational and loading tests. The results are as follows:

(1) The test rig provided with magnetic bearings has proved to attain its stable rotating characteristics with low vibration. It has also demonstrated sufficient capability to withstand the fluid force at work at the time of the loading tests up to the overspeed corresponding to 120 % of the rated revolutions of the turbine, either as operated with the analog controller or with the digital controller.

(2) Even with the digital controller by the PID control process, it was possible to attain the same performance in control as with the analog controller.

(3) When any notch filter is used to prevent vibration in the shaft bending mode, it increases the margin of capability of accommodating changes in the natural frequency of the shaft system to set the central frequency for the notch filter at a level somewhat lower than that of the natural frequency at the time of its standstill.

(4) Since the vibration characteristics of magnetic bearings undergo changes when fluid force works on the bearings, it is necessary to perform sufficient simulations in advance with respect to such changes.

References:

[1] KIRK, R. G., HUSTAK, J. F. and SCHOENECK, K. A.: Analysis and Test Results of Two Centrifugal Compressors Using Active Magnetic Bearings. IMechE C278/88, pp. 93-, 1988

[2] BLEULER, H. and SALM, J.: Active Electromagnetic Suspension and Vibration Control of a Signal Processor. IMechE C287/88, pp. 101-, 1988

[3] MATSUSHITA, O.: Stabilization by Cross Stiffness Control of Electromagnetic Damper for Contained Liquid Rotor Unstable Vibration. Intern. Cont. on Vibration in Rotating Machinery, Sep., pp. 13-15, 1988

[4] MATSUSHITA, O., YOSHIDA, T., TAKAGI, T., and TAKAHASHI, N.: Rotor Vibration Simulation with Active Magnetic Bearing Control. 2nd Intern. Sympo., MAGNETIC BEARINGS, July, pp. 12-14, 1990, Tokyo, Japan